NUCL SCI TECH (2017) 28:86
DOI 10.1007/s41365-017-0239-2

A theoretical study on different cluster configurations of the ^{9}Be nucleus by using a simple cluster model

M. Aygun[1] · Z. Aygun[2]

Received: 7 December 2016 / Revised: 8 February 2017 / Accepted: 12 February 2017 / Published online: 6 May 2017

Abstract In this study, a comprehensive investigation on different cluster configurations of the ^{9}Be nucleus is performed with a simple cluster approach. With this goal, the elastic scattering angular distributions of ^{9}Be by ^{27}Al, ^{28}Si, ^{64}Zn, ^{144}Sm, ^{208}Pb, and ^{209}Bi target nuclei are reanalyzed for $\alpha + \alpha + n$, $d + {}^{7}Li$, ${}^{3}H + {}^{6}Li$, ${}^{3}He + {}^{6}He$ and $n + {}^{8}Be$ cluster configurations of the ^{9}Be projectile within the framework of the optical model. The theoretical results are compared with each other as well as the experimental data. The results provide an opportunity for a test of different cluster configurations in explaining the elastic scattering of ^{9}Be nucleus.

Keywords Cluster structure · Optical model · Double folding model · Elastic scattering

1 Introduction

Cluster structure is an important feature observed in both stable and unstable nuclei. For example, ^{11}Li, known as a halo nucleus, is considered as a core (^{9}Li) and two-valence neutrons [1]. Or in stable nuclei, it is assumed that ^{12}C and ^{16}O nuclei have a α cluster structure. A large number of experimental and theoretical studies have been carried out to examine the cluster structures of nuclei [2–5]. Experimental techniques have been applied to display cluster cases in nuclei. For theoretical analysis, the Bloch-Brink α-cluster model (ACM), the antisymmetrized molecular dynamics (AMD), and the generator coordinate method (GCM) have been improved [6]. Therefore, it can be said that the cluster feature of a nucleus is an important parameter to examine the structure of a nucleus, to study cluster decay, break-up reactions, and stellar nucleosynthesis, to constitute different configurations with elements, and to understand the processes in nuclear astrophysics [7–9].

Recently, Aygun [10] applied a simple cluster method to a ^{12}Be nucleus. He investigated different cluster structures of the ^{12}Be nucleus within the optical model (OM). He reported the theoretical results in explaining the experimental data. We think that this simple method will be interesting in applying different nuclei. With this goal, in the present study, we focus on the theoretical analysis of the existing cluster models of the ^{9}Be nucleus over literature.

In this work, we investigate $\alpha + \alpha + n$, $d + {}^{7}Li$, ${}^{3}H + {}^{6}Li$, ${}^{3}He + {}^{6}He$, and $n + {}^{8}Be$ [11–13] structure models of the ^{9}Be nucleus in terms of a simple cluster model. We obtain elastic scattering angular distributions of ^{9}Be by ^{27}Al, ^{28}Si, ^{64}Zn, ^{144}Sm, ^{208}Pb, and ^{209}Bi target nuclei by using the double folding (DF) model based on the OM. We compare the theoretical results with the experimental data. Thus, the similarities and differences between cluster models applied in the calculations of ^{9}Be nucleus are determined.

In the next section, a brief description of theoretical calculation is given. The results and discussion are defined in Sect. 3. Section 4 is devoted to our summary and conclusions.

✉ M. Aygun
maygun@beu.edu.tr

1 Department of Physics, Bitlis Eren University, Bitlis 13000, Turkey

2 Vocational School of Technical Sciences, Bitlis Eren University, Bitlis 13000, Turkey

2 The calculation process

2.1 The optical model

The optical potential, which consists of real ($V(r)$) and imaginary ($W(r)$) potentials, is parameterized by

$$V_{\text{optical}}(r) = V(r) + iW(r). \tag{1}$$

To determine the real part of the optical potential, the DF model is used. The DF potential is obtained by means of the density distributions of projectiles and target together with an effective nucleon–nucleon interaction potential (v_{NN}). In this manner, the DF potential is shown by

$$V_{\text{DF}}(\mathbf{r}) = \int \mathrm{d}\mathbf{r}_1 \int \mathrm{d}\mathbf{r}_2 \rho_P(\mathbf{r}_1)\rho_T(\mathbf{r}_2) v_{\text{NN}}(\mathbf{r}_{12}), \tag{2}$$

where $\mathbf{r}_{12} = \mathbf{r} - \mathbf{r}_1 + \mathbf{r}_2$, $v_{\text{NN}}(\mathbf{r}_{12})$ is the effective NN interaction, and $\rho_P(\mathbf{r}_1)$ and $\rho_T(\mathbf{r}_2)$, respectively, are the density distributions of projectile and target.

In order to make a comparative study, we have used five different density distributions for the ^{9}Be nucleus. Each of these densities is explained in the following. On the other hand, for the densities of ^{27}Al, ^{28}Si, ^{208}Pb, and ^{209}Bi target nuclei, two-parameter Fermi (2pF) density distribution has been used, which is given by

$$\rho(r) = \frac{\rho_0}{1 + \exp\left(\frac{r-c}{z}\right)}. \tag{3}$$

ρ_0, c, and z parameters are presented in Table 1.

The density distributions of ^{64}Zn and ^{144}Sm target nuclei are taken from the Hartree-Fock-Bogolubov (HFB) method based on the BSk2 Skyrme force [17].

For v_{NN}, we have used the most common one, the M3Y nucleon–nucleon (Michigan 3 Yukawa) realistic interaction, which is formulated as

$$v_{\text{NN}}(r) = 7999\frac{\exp(-4r)}{4r} - 2134\frac{\exp(-2.5r)}{2.5r} + J_{00}(E)\delta(r)\text{MeV}, \tag{4}$$

where $J_{00}(E)$ is the exchange term given by

$$J_{00}(E) = 276\ (1 - 0.005\ E_{\text{Lab}}/A_{\text{P}})\text{MeVfm}^3, \tag{5}$$

where E_{Lab} and A_{P} are the laboratory energy and mass number of the projectile, respectively. Finally, the imaginary part of the optical potential is assumed in Woods–Saxon (WS) form

$$W(r) = W_0 f(r, R_w, a_w), \tag{6}$$

$$f(r, R_w, a_w) = [1 + \exp(X)]^{-1}, \quad X = (r - R_w)/a_w, \tag{7}$$

where $R_w = r_w\ (A_{\text{P}}^{1/3} + A_{\text{T}}^{1/3})$ and A_{P} and A_{T} are the mass numbers of the projectile and target nuclei, respectively. The code FRESCO has been used in OM calculations [18].

Table 1 The parameters of 2pF density distributions of ^{27}Al, ^{28}Si, ^{208}Pb, and ^{209}Bi nuclei

2pF				
Nucleus	c (fm)	z (fm)	ρ_0 (fm)$^{-3}$	References
^{27}Al	2.84	0.569	0.2015	[14]
^{28}Si	3.15	0.475	0.175	[15]
^{208}Pb	6.62	0.551	0.1600	[14]
^{209}Bi	6.75	0.468	0.154887	[16]

2.2 Simple parametrization of structure models of ^{9}Be nucleus

Here, various cluster models of the ^{9}Be are evaluated within a different approach. With this goal, it is assumed that ^{9}Be nucleus consists of $\alpha + \alpha + \text{n}$, $\text{d} + {}^7\text{Li}$, $^3\text{H} + {}^6\text{Li}$, $^3\text{He} + {}^6\text{He}$, and $\text{n} + {}^8\text{Be}$ systems. The density distributions of ^{9}Be for these models are obtained and applied to produce the real potential in the DF model calculations based on the OM. However, the imaginary part of the optical potential is taken as the WS potential. The theoretical calculation of each system is conducted in the same form. We should say that we have not obtained a new density distribution. We have used the existing density distributions in the literature with only a simple approach.

2.2.1 $\alpha + \alpha + \text{n}$ *system*

Firstly, we concentrate on the $\alpha + \alpha + \text{n}$ cluster structure of the ^{9}Be nucleus. In this manner, we assume the density distribution of ^{9}Be in the following form

$$\rho_{^9\text{Be}}(r) = \rho_\alpha(r) + \rho_\alpha(r) + \rho_{\text{n}}(r). \tag{8}$$

We use different density distributions for each α density. These densities, respectively, are

$$\rho_\alpha(r) = 0.4229\ \exp(-0.7024r^2) \tag{9}$$

and

$$\rho_\alpha(r) = 4\left(\frac{3\pi b^2}{4}\right)^{-3/2} \exp\left(-\frac{4r^2}{3b^2}\right), \tag{10}$$

where $b = 1.28$ fm [15, 19]. The density distribution of 1n-halo is given by [20, 21]

$$\rho_{\text{n}}(r) = \left(\frac{1}{\gamma\sqrt{\pi}}\right)^3 \exp(-r^2/\gamma^2), \tag{11}$$

where γ is adjusted to reproduce the experimental value for the rms radius of ^{9}Be.

Table 2 The N_R values obtained with the DF calculations for $\alpha+\alpha+n$, $d+{}^7$Li, ^{3}H + ^{6}Li, ^{3}He + ^{6}He, and n + ^{8}Be cluster structures of the ^{9}Be nucleus in the analysis of the ^{9}Be + ^{27}Al, ^{28}Si, ^{64}Zn, ^{144}Sm, ^{208}Pb and ^{209}Bi reactions

System	Energy (MeV)	N_R				
		$\alpha+\alpha+n$	$d+{}^7$Li	^{3}H + ^{6}Li	^{3}He + ^{6}He	n + ^{8}Be
^{9}Be + ^{27}Al	22	0.66	0.96	0.67	0.56	0.40
	25	0.63	0.80	0.68	0.50	0.41
	32	1.00	1.00	1.00	0.84	0.82
	35	1.00	1.03	1.00	0.75	0.83
	13	0.82	1.09	1.00	0.66	0.55
^{9}Be + ^{28}Si	17	0.67	1.06	0.865	0.53	0.46
	23	0.81	1.064	1.00	0.67	0.63
	26	0.95	1.07	1.03	0.86	0.74
	30	0.978	1.07	1.00	0.88	0.80
^{9}Be + ^{64}Zn	21	0.66	0.90	0.70	0.50	0.40
	23	0.575	0.66	0.58	0.435	0.33
	26	0.50	0.56	0.50	0.36	0.29
	28	0.69	0.83	0.84	0.53	0.47
^{9}Be + ^{144}Sm	39	0.716	0.85	0.73	0.53	0.40
	41	0.745	0.93	0.78	0.55	0.43
	44	0.733	0.92	0.79	0.54	0.443
	48	0.78	1.00	0.90	0.60	0.48
^{9}Be + ^{208}Pb	40	0.950	1.04	1.000	0.78	0.650
	42	0.680	0.78	0.715	0.525	0.425
	47.2	0.678	0.765	0.690	0.515	0.420
	50	0.77	0.83	0.810	0.58	0.500
	39	1.16	1.36	1.21	1.00	0.91
^{9}Be + ^{209}Bi	40	1.17	1.15	1.30	0.98	0.88
	42	0.94	1.00	1.00	0.69	0.63
	44	0.645	0.80	0.62	0.51	0.51

2.2.2 *d+*^{7}Li *system*

Secondly, the density distribution of ^{9}Be projectile is obtained as the sum of densities of d and ^{7}Li nuclei shown by

$$\rho_{^9\mathrm{Be}}(r) = \rho_{\mathrm{d}}(r) + \rho_{^7\mathrm{Li}}(r). \tag{12}$$

In this way, the density of d is in the following form

$$\rho_{\mathrm{d}}(r) = \rho_0 \exp(-\varrho r^2), \tag{13}$$

where $\rho_0 = 0.0992\ \mathrm{fm}^{-3}$ and $\varrho = 0.424\ \mathrm{fm}^{-2}$ [22]. ^{7}Li density is parameterized as [23]

$$\rho_{^7\mathrm{Li}}(r) = 0.1387(1+0.1673r^2)\exp(-0.3341r^2). \tag{14}$$

2.2.3 ^{3}H + ^{6}Li *system*

The ^{9}Be nucleus can be considered as a cluster form of ^{3}H and ^{6}Li nuclei. In this manner, ^{9}Be density is taken as

$$\rho_{^9\mathrm{Be}}(r) = \rho_{^3\mathrm{H}}(r) + \rho_{^6\mathrm{Li}}(r). \tag{15}$$

^{3}H density distribution is evaluated as the variational Monte Carlo (VMC) density obtained by using the Argonne v18 (AV18) two-nucleon and Urbana X three-nucleon potentials (AV18+UX) [24]. However, ^{6}Li density is conducted as [25]

$$\rho_{^6\mathrm{Li}}(r) = 0.203\exp(-0.3306r^2) + (-0.0131+0.001378r^2)\exp(-0.1584r^2). \tag{16}$$

2.2.4 ^{3}He + ^{6}He *system*

Another cluster structure of the ^{9}Be nucleus is in the form of ^{3}He and ^{6}He nuclei. Thus, ^{9}Be density can be written as

$$\rho_{^9\mathrm{Be}}(r) = \rho_{^3\mathrm{He}}(r) + \rho_{^6\mathrm{He}}(r). \tag{17}$$

^{3}He density distribution is given by [26]

$$\rho_{^3\mathrm{He}}(r) = 0.2201\exp(-0.5505r^2). \tag{18}$$

Table 3 The W_0 values of the imaginary potential for $\alpha+\alpha+n$, $d+{}^7Li$, ${}^3H+{}^6Li$, ${}^3He+{}^6He$, and $n+{}^8Be$ cluster configurations of the ${}^9Be$ nucleus in the analysis of the ${}^9Be+{}^{27}Al$, ${}^{28}Si$, ${}^{64}Zn$, ${}^{144}Sm$, ${}^{208}Pb$, and ${}^{209}Bi$ reactions

System	Energy (MeV)	W_0 (MeV)				
		$\alpha+\alpha+n$	$d+{}^7Li$	${}^3H+{}^6Li$	${}^3He+{}^6He$	$n+{}^8Be$
${}^9Be+{}^{27}Al$	22	18.70	15.00	15.70	17.6	19.00
	25	18.90	15.30	15.80	20.6	20.00
	32	19.00	15.50	16.00	21.6	30.00
	35	23.40	18.50	20.75	22.6	30.70
${}^9Be+{}^{28}Si$	13	7.00	12.90	9.90	9.00	7.70
	17	16.90	14.00	15.90	16.90	16.90
	23	17.00	14.10	16.20	17.60	19.10
	26	20.00	14.20	16.30	25.50	24.00
	30	22.00	14.30	16.80	26.80	27.10
${}^9Be+{}^{64}Zn$	21	10.10	12.20	12.50	11.30	11.45
	23	10.20	12.30	12.60	8.80	11.50
	26	10.40	13.00	13.00	10.80	12.00
	28	10.70	13.50	15.50	12.80	12.50
${}^9Be+{}^{144}Sm$	39	10.00	13.00	12.80	11.30	13.00
	41	10.94	15.40	14.00	12.00	14.00
	44	10.96	16.00	14.50	12.50	15.00
	48	12.00	16.10	15.00	13.00	16.00
${}^9Be+{}^{208}Pb$	40	12.00	16.50	14.85	13.00	12.50
	42	15.50	18.00	17.00	16.10	16.10
	47.2	18.00	21.00	21.00	19.00	18.50
	50	19.00	21.70	22.30	20.30	20.30
${}^9Be+{}^{209Bi}$	39	10.00	16.00	13.90	10.40	8.90
	40	10.20	18.10	14.00	10.80	9.00
	42	12.20	18.30	15.40	14.20	11.90
	44	16.50	19.90	20.10	16.90	13.90

In all the calculations, the Coulomb radius (R_c), r_w, and a_w values have been fixed as 1.25, 1.27, and 0.75, respectively

${}^6He$ density is evaluated in the following form

$$\rho_{^6He}(r)=\rho_0\exp(-\beta r^2), \tag{19}$$

where β is adjusted to reproduce the experimental value for the rms radius of the ${}^6He = 2.54$ fm. ρ_0 can be obtained from the normalization condition

$$\int\rho(r)r^2\mathrm{d}r=\frac{A}{4\pi}, \tag{20}$$

where A is the mass number.

2.2.5 *n* + ^{8}Be *system*

Finally, the ${}^9Be$ nucleus is thought as a n + ${}^8Be$ cluster model. Thus, ${}^9Be$ density is the sum of n and ${}^8Be$ densities parameterized as

$$\rho_{^9Be}(r)=\rho_n(r)+\rho_{^8Be}(r). \tag{21}$$

The density distribution of 1n-halo is the same as Eq. (11). The VMC density distribution for the ${}^8Be$ nucleus is used [24].

3 Results and discussion

We have investigated $\alpha+\alpha+n$, $d+{}^7Li$, ${}^3H+{}^6Li$, ${}^3He+{}^6He$, and n + ${}^8Be$ cluster configurations known for ${}^9Be$ by using the DF model based on the OM. In this context, we have analyzed the elastic scattering data of six different nuclear reactions which consist of ${}^{27}Al$, ${}^{28}Si$, ${}^{64}Zn$, ${}^{144}Sm$, ${}^{208}Pb$, and ${}^{209}Bi$ nuclei, in order to make a comparative study of the interactions with light, medium, and heavy target nuclei of ${}^9Be$. For a more comprehensive analysis, we have also investigated the elastic scattering data for different incident energies that can be obtained from the literature of the reactions analyzed with this work. While the real potential is obtained via the DF model, the

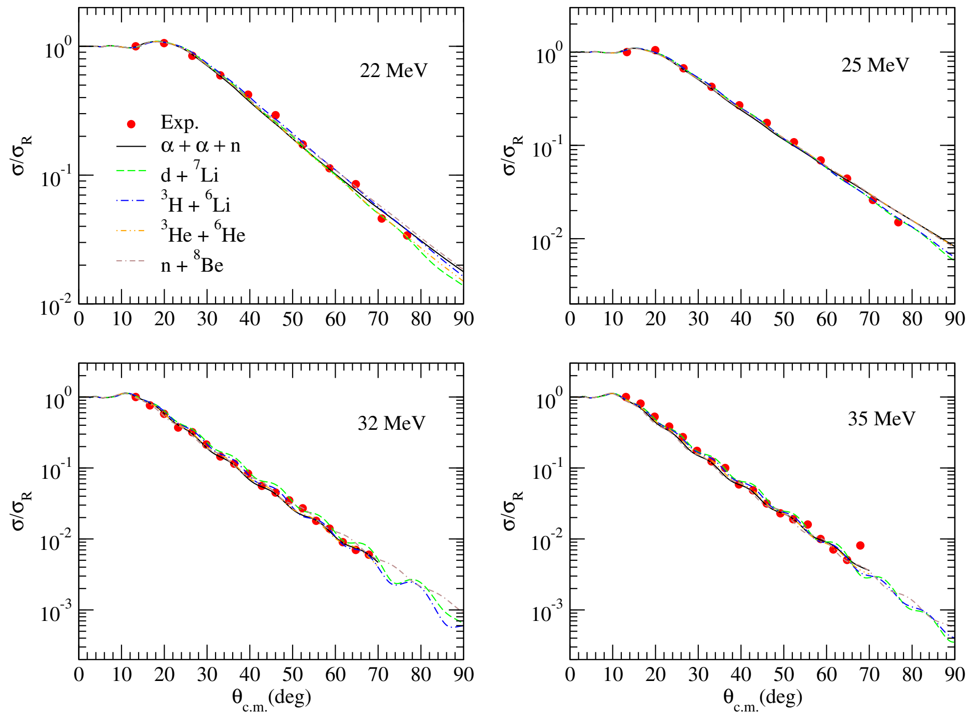

Fig. 1 (Color online) The elastic scattering angular distributions for $\alpha+\alpha+\mathrm{n}$, $\mathrm{d}+{}^{7}\mathrm{Li}$, ${}^{3}\mathrm{H}+{}^{6}\mathrm{Li}$, ${}^{3}\mathrm{He}+{}^{6}\mathrm{He}$, and $\mathrm{n}+{}^{8}\mathrm{Be}$ cluster configurations of ^{9}Be in the analysis of the ${}^{9}\mathrm{Be}+{}^{27}\mathrm{Al}$ system in comparison with the experimental data at 22, 25, 32, and 35 MeV. The experimental data are from Refs. [27–29]

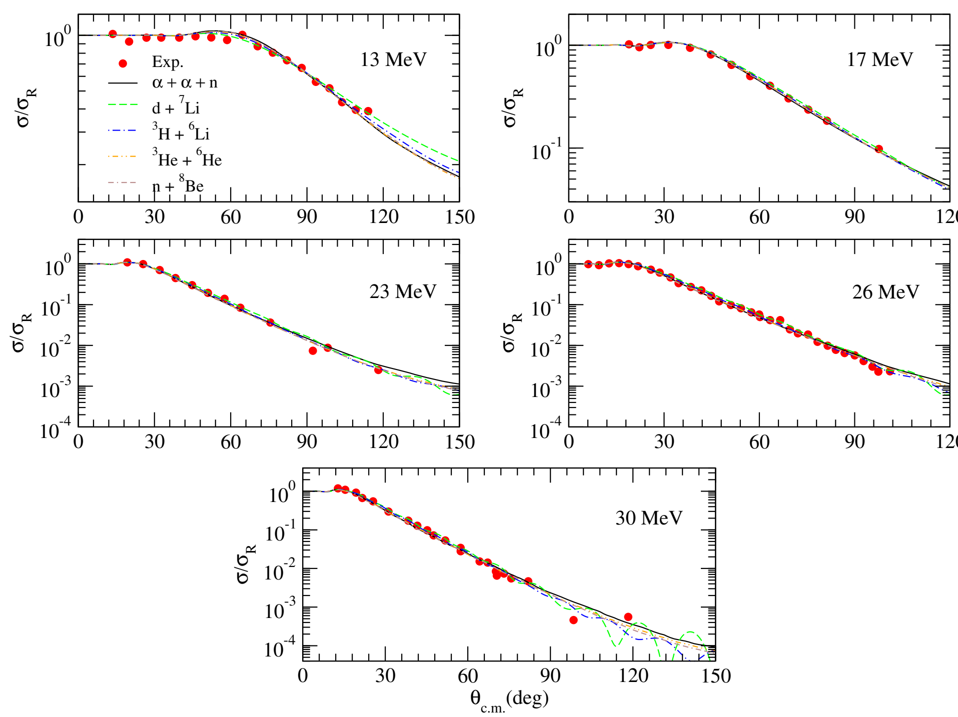

Fig. 2 (Color online) The elastic scattering angular distributions for $\alpha+\alpha+\mathrm{n}$, $\mathrm{d}+{}^{7}\mathrm{Li}$, ${}^{3}\mathrm{H}+{}^{6}\mathrm{Li}$, ${}^{3}\mathrm{He}+{}^{6}\mathrm{He}$, and $\mathrm{n}+{}^{8}\mathrm{Be}$ cluster cases of ^{9}Be in the analysis of the ${}^{9}\mathrm{Be}+{}^{28}\mathrm{Si}$ system in comparison with the experimental data at 13, 17, 23, 26, and 30 MeV. The experimental data are from Refs. [29–31]

imaginary potential has been assumed as WS potential. To acquire good agreement results with the experimental data, we have researched the normalization constant (N_{R}) for the real part and W_0, r_w, a_w potential parameters for the imaginary part. In this context, the values of N_{R} and W_0, r_w, a_w parameters are listed in Tables 2 and 3, respectively.

Elastic scattering of the ${}^{9}\mathrm{Be}+{}^{27}\mathrm{Al}$ reaction has been investigated for $\alpha+\alpha+\mathrm{n}$, $\mathrm{d}+{}^{7}\mathrm{Li}$, ${}^{3}\mathrm{H}+{}^{6}\mathrm{Li}$, ${}^{3}\mathrm{He}+{}^{6}\mathrm{He}$,

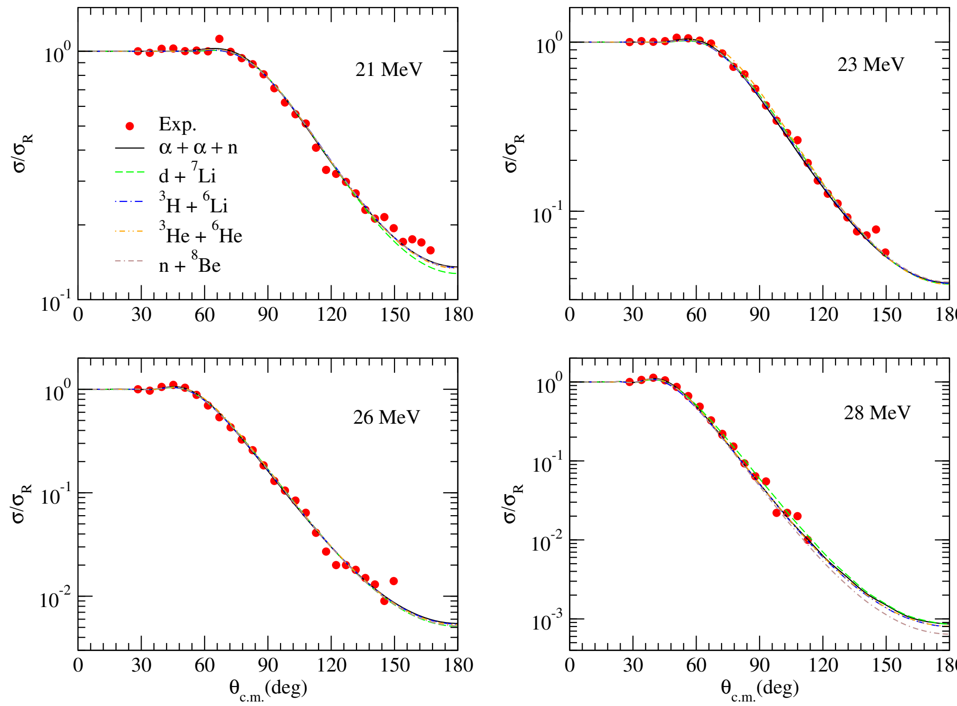

Fig. 3 (Color online) The elastic scattering angular distributions for $\alpha + \alpha + n$, $d + {}^{7}Li$, ${}^{3}H + {}^{6}Li$, ${}^{3}He + {}^{6}He$, and $n + {}^{8}Be$ cluster structures of ${}^{9}Be$ in the analysis of the ${}^{9}Be + {}^{64}Zn$ system in comparison with the experimental data at 21, 23, 26, and 28 MeV. The experimental data are from Refs. [29, 32]

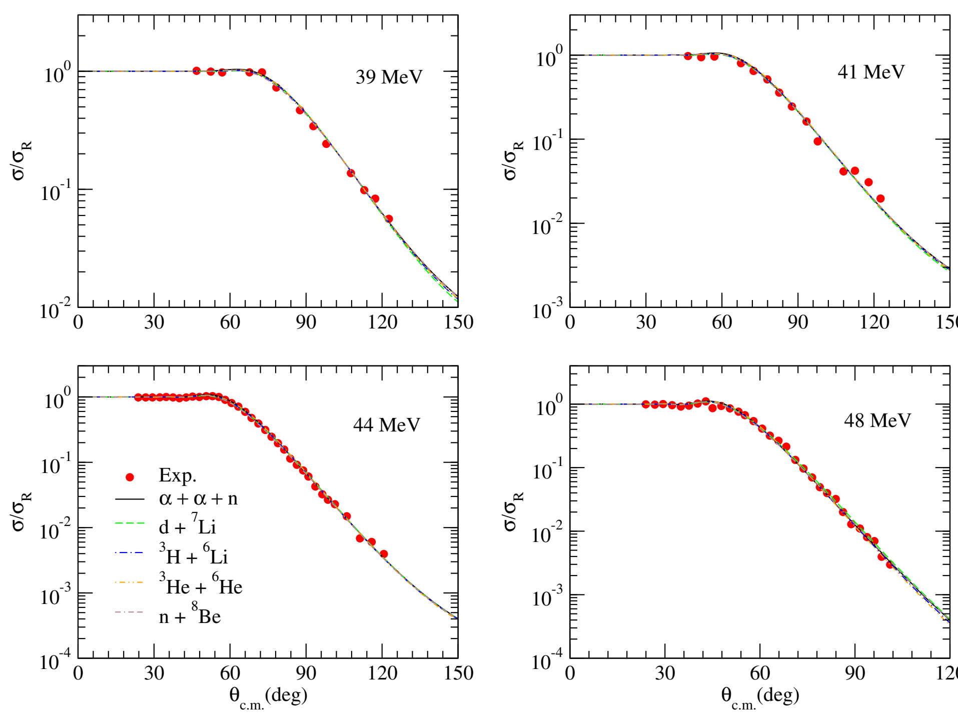

Fig. 4 (Color online) The elastic scattering angular distributions for $\alpha + \alpha + n$, $d + {}^{7}Li$, ${}^{3}H + {}^{6}Li$, ${}^{3}He + {}^{6}He$, and $n + {}^{8}Be$ cluster models of ${}^{9}Be$ in the analysis of the ${}^{9}Be + {}^{144}Sm$ system in comparison with the experimental data at 39, 41, 44, and 48 MeV. The experimental data are from Refs. [29, 33, 34]

and $n + {}^{8}Be$ cluster systems at 22, 25, 32, and 35 MeV. The results shown in Fig. 1 have been compared with each other as well as the experimental data. It has been seen that all the theoretical results are in very good agreement with the data.

Angular distributions of elastic scattering of ${}^{9}Be$ on ${}^{28}Si$ have been studied for five different cluster configurations at incident energies of 13, 17, 23, 26, and 30 MeV. The theoretical results are plotted comparatively in Fig. 2. It has been observed that the results have displayed an agreement behavior with the data.

Elastic scattering of the ${}^{9}Be + {}^{64}Zn$ reaction has been analyzed for $\alpha + \alpha + n$, $d + {}^{7}Li$, ${}^{3}H + {}^{6}Li$, ${}^{3}He + {}^{6}He$, and $n + {}^{8}Be$ cluster cases at 21, 23, 26, and 28 MeV. In this

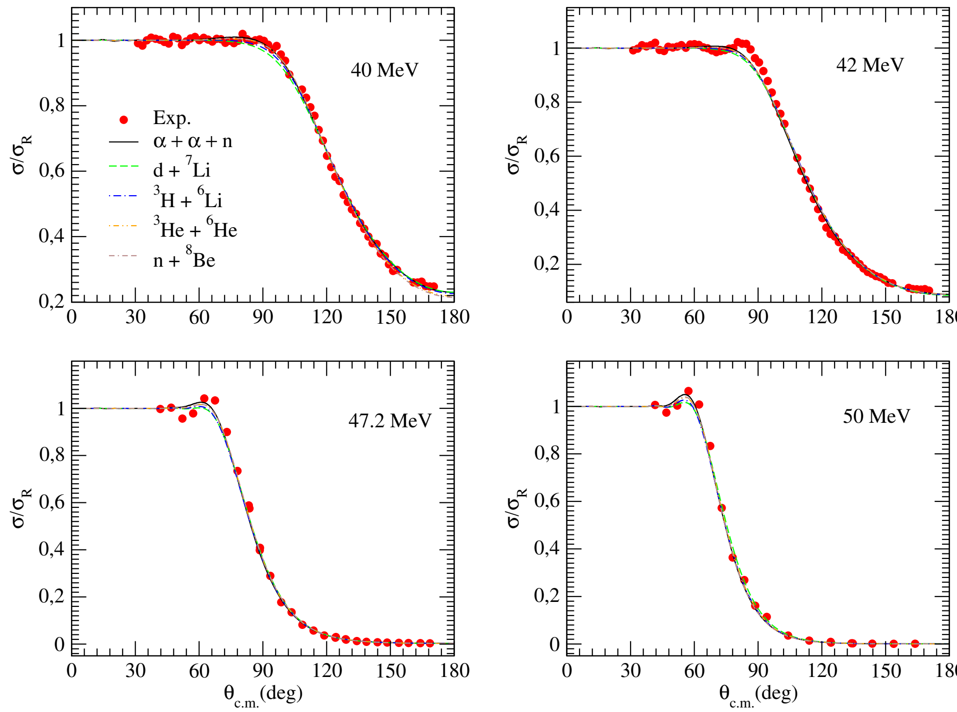

Fig. 5 (Color online) The elastic scattering angular distributions for $\alpha + \alpha + n$, $d + {}^7Li$, ${}^3H + {}^6Li$, ${}^3He + {}^6He$, and $n + {}^8Be$ cluster cases of ^{9}Be in the analysis of the $^9Be + {}^{208}Pb$ system in comparison with the experimental data at 40, 42, 47.2, and 50 MeV. The experimental data are from Ref. [35]

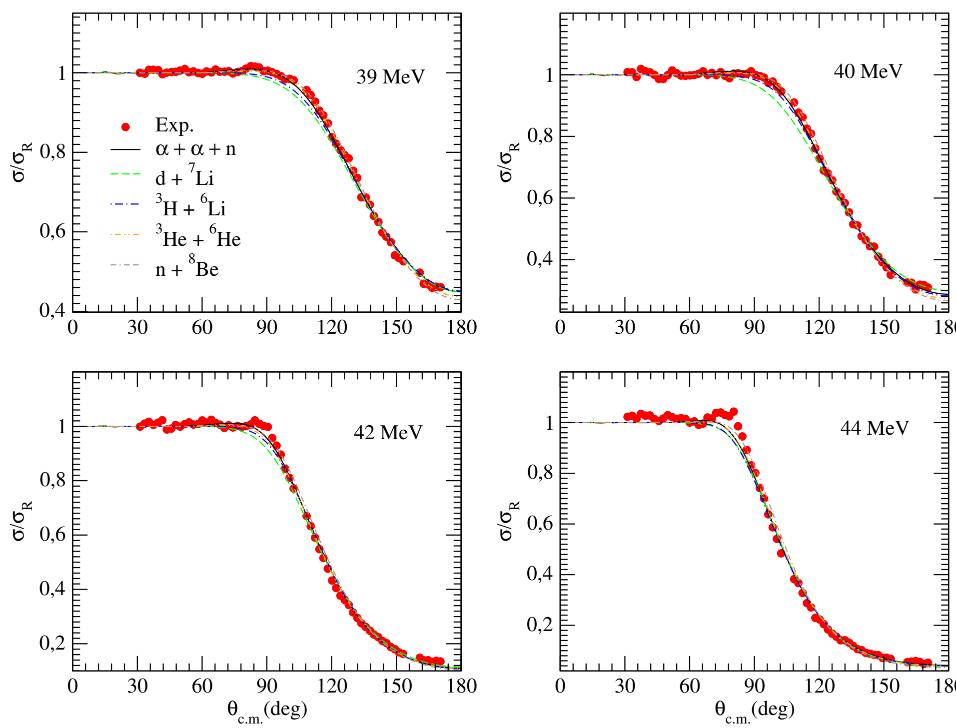

Fig. 6 (Color online) The elastic scattering angular distributions for $\alpha + \alpha + n$, $d + {}^7Li$, ${}^3H + {}^6Li$, ${}^3He + {}^6He$, and $n + {}^8Be$ cluster configurations of ^{9}Be in the analysis of the $^9Be + {}^{209}Bi$ system in comparison with the experimental data at 39, 40, 42, and 44 MeV. The experimental data are from Refs. [29, 35]

context, the results are shown in Fig. 3. Agreement between theoretical results and experimental data is very good. Also, our results display very similar behavior to each other.

^{9}Be elastic scattering by ^{144}Sm has been examined by using the DF model at 39, 41, 44, and 48 MeV. As seen from Fig. 4, agreement of the theoretical results with the data is almost excellent.

As heavy target nuclei, elastic scattering angular distributions of $^9Be + {}^{208}Pb$ (at 40, 42, 47.2, and 50 MeV) and $^9Be + {}^{209}Bi$ (at 39, 40, 42, and 44 MeV) reactions have been investigated for $\alpha + \alpha + n$, $d + {}^7Li$, ${}^3H + {}^6Li$,

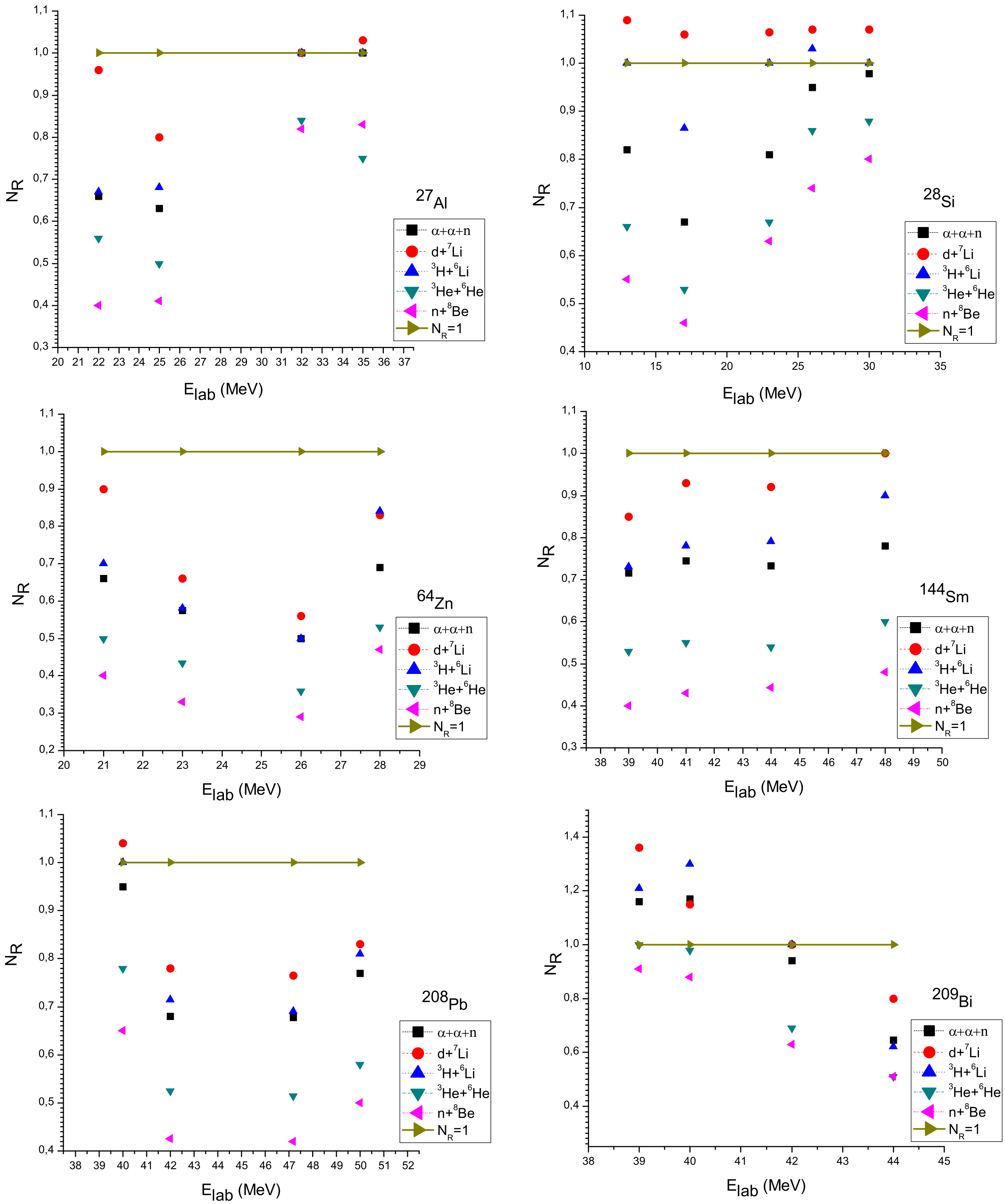

Fig. 7 (Color online) The N_R changes as a function of incident energy for $\alpha+\alpha+n$, $d+{}^{7}Li$, ${}^{3}H+{}^{6}Li$, ${}^{3}He+{}^{6}He$, and $n+{}^{8}Be$ cluster cases of each system examined with this work. The *solid line* shown with $N_R = 1$ is to guide the eye

Table 4 The σ values obtained for $\alpha+\alpha+n$, $d+{}^{7}Li$, $^{3}H+{}^{6}Li$, $^{3}He+{}^{6}He$, and $n+{}^{8}Be$ cluster cases in the analysis of the $^{9}Be+{}^{27}Al$, ^{28}Si, ^{64}Zn, ^{144}Sm, ^{208}Pb, and ^{209}Bi reactions

System	Energy (MeV)	σ (mb)				
		$\alpha+\alpha+n$	$d+{}^{7}Li$	$^{3}H+{}^{6}Li$	$^{3}He+{}^{6}He$	$n+{}^{8}Be$
$^{9}Be+{}^{27}Al$	22	1413.3	1377.9	1361.8	1400.5	1412.9
	25	1536.4	1488.3	1487.2	1561.2	1554.3
	32	1758.7	1694.7	1706.4	1802.2	1921.8
	35	1876.2	1798.6	1834.0	1859.5	1984.6
$^{9}Be+{}^{28}Si$	13	366.4	437.2	412.4	399.1	384.0
	17	965.8	934.2	956.9	963.5	968.8
	23	1377.9	1334.8	1372.6	1390.6	1425.9
	26	1558.9	1458.7	1498.7	1639.8	1626.7
	30	1709.7	1579.0	1623.1	1780.0	1792.1
$^{9}Be+{}^{64}Zn$	21	384.3	414.5	412.7	398.2	400.6
	23	593.4	623.9	628.9	558.1	610.7
	26	860.8	910.9	910.1	863.1	891.4
	28	1046.9	1102.4	1146.8	1088.9	1094.1
$^{9}Be+{}^{144}Sm$	39	762.0	818.1	812.8	784.7	816.7
	41	944.3	1028.7	1000.9	960.7	1001.6
	44	1147.6	1251.8	1222.6	1177.5	1234.0
	48	1411.0	1500.0	1480.6	1432.0	1497.5
$^{9}Be+{}^{208}Pb$	40	297.3	335.3	322.3	308.5	304.8
	42	511.7	533.3	522.6	514.2	515.1
	47.2	1021.8	1053.4	1055.9	1030.6	1024.0
	50	1264.2	1286.8	1303.2	1276.3	1282.4
$^{9}Be+{}^{209}Bi$	39	164.0	207.6	192.4	167.2	155.6
	40	239.3	304.7	274.3	245.7	228.1
	42	428.4	488.6	461.2	449.7	421.1
	44	659.5	694.5	696.9	661.3	624.7

$^{3}He+{}^{6}He$, and $n+{}^{8}Be$ cluster configurations of ^{9}Be by using the DF model. The theoretical results are plotted in Fig. 5 for $^{9}Be+{}^{208}Pb$ and in Fig. 6 for $^{9}Be+{}^{209}Bi$. The results for both $^{9}Be+{}^{208}Pb$ and $^{9}Be+{}^{209}Bi$ systems are in good agreement with the data.

It is well known that N_R, when applied to obtain good agreement results with the data, shows the success of the DF model [36]. With this goal, to evaluate the results of $\alpha+\alpha+n$, $d+{}^{7}Li$, $^{3}H+{}^{6}Li$, $^{3}He+{}^{6}He$, and $n+{}^{8}Be$ cluster configurations from another angle, we have shown the N_R values for all the systems investigated in Table 2. Also, changes of N_R values for the systems are plotted comparatively in Fig. 7. We have observed that N_R values of d+^{7}Li and $^{3}H+{}^{6}Li$ cases are close to each other and are better than the N_R values of the other systems. However, the worst N_R values have been found for the $n+{}^{8}Be$ cluster case. As a result of this, we can say that $\alpha+\alpha+n$, $d+{}^{7}Li$, and $^{3}H+{}^{6}Li$ cluster cases are more suitable within different cluster configurations of the ^{9}Be nucleus.

In the present research, we have given the reaction cross sections (σ) of the systems analyzed in Table 4. When we have examined the results, we have observed that d+^{7}Li and $^{3}H+{}^{6}Li$ cluster cases have given very close values to each other. Also, we have noticed that d+^{7}Li and $^{3}H+{}^{6}Li$ cluster structures have a larger cross section than the other systems.

As another comparison parameter of $\alpha+\alpha+n$, $d+{}^{7}Li$, $^{3}H+{}^{6}Li$, $^{3}He+{}^{6}He$, and $n+{}^{8}Be$ cluster cases, we have investigated χ^2/N values. With this goal, we have calculated χ^2/N values for each system according to the experimental error of around 10% and have listed the results in Table 5. We have observed that the χ^2/N values are rather small in a general sense.

4 Summary and conclusions

We have reported the study of different cluster configurations of ^{9}Be investigated by terms of a simple cluster method. With this goal, we have performed a different and new study to determine which cluster configurations of ^{9}Be are more valid. The theoretical analysis has been carried

Table 5 The χ^2/N values calculated for $\alpha+\alpha+n$, $d+{}^7Li$, ${}^3H+{}^6Li$, ${}^3He+{}^6He$, and $n+{}^8Be$ cluster structures in the analysis of the ${}^9Be+{}^{27}Al$, ${}^{28}Si$, ${}^{64}Zn$, ${}^{144}Sm$, ${}^{208}Pb$, and ${}^{209}Bi$ reactions

System	Energy (MeV)	χ^2/N				
		$\alpha+\alpha+n$	$d+{}^7Li$	${}^3H+{}^6Li$	${}^3He+{}^6He$	$n+{}^8Be$
${}^9Be+{}^{27}Al$	22	0.7106	0.4661	0.5072	0.5526	0.8924
	25	1.2267	0.3399	0.3888	1.1110	1.0784
	32	0.7702	2.8317	0.8422	0.7360	1.2528
	35	2.7976	3.7862	2.8590	2.5997	3.2359
${}^9Be+{}^{28}Si$	13	0.3192	0.1815	0.1896	0.2674	0.2681
	17	0.1268	0.3231	0.1644	0.1236	0.1160
	23	6.5501	7.5186	3.1606	3.2760	3.4991
	26	2.8418	2.5614	0.9783	1.9139	1.8879
	30	21.423	10.984	9.5054	13.561	12.561
${}^9Be+{}^{64}Zn$	21	0.3289	0.5345	0.3735	0.3862	0.3564
	23	0.3722	0.3136	0.3317	0.3823	0.2922
	26	1.5801	1.7245	1.6326	1.7803	1.6315
	28	1.7144	1.9992	2.0108	1.6673	2.5068
${}^9Be+{}^{144}Sm$	39	0.4279	0.4839	0.4126	0.4696	0.2974
	41	1.9833	1.9756	1.9868	2.2124	1.7976
	44	0.4520	0.4675	0.4194	0.5638	0.3572
	48	0.8970	0.9888	0.7446	0.8173	0.8738
${}^9Be+{}^{208}Pb$	40	0.0358	0.0568	0.0450	0.0553	0.0727
	42	0.1251	0.2156	0.1847	0.1461	0.1605
	47.2	0.4213	0.6075	0.4933	0.4574	0.5412
	50	3.0902	2.2716	2.9785	2.7373	4.5775
${}^9Be+{}^{209}Bi$	39	0.0167	0.0464	0.0306	0.0108	0.0165
	40	0.0284	0.0987	0.0417	0.0516	0.0897
	42	0.1852	0.1645	0.2286	0.1973	0.3453
	44	0.3487	0.6098	0.3950	0.4912	1.2496

out for $\alpha+\alpha+n$, $d+{}^7Li$, ${}^3H+{}^6Li$, ${}^3He+{}^6He$, and $n+{}^8Be$ cluster cases by using the DF model within the scope of the OM. The elastic scattering results for each system have been plotted in figures. Also, N_R values, the optical potential parameters, cross sections, and χ^2/N values have been listed in tables. It has been seen that our results are in very good harmony with the experimental data in general sense. However, the $\alpha+\alpha+n$, $d+{}^7Li$, and ${}^3H+{}^6Li$ results are close to each other and are better than the results of the other cluster cases. Additionally, we have noticed that the $\alpha+\alpha+n$, $d+{}^7Li$, and ${}^3H+{}^6Li$ results are more compatible with the experimental data. However, we should say that the ${}^3H+{}^6Li$ results are in more harmony with the data according to χ^2/N values.

Consequently, we have applied a different and simple approach to the analysis of the internal structure of the ${}^9Be$ nucleus within the framework of the DF model. We should say that we do not claim very precise results. We have observed that this method has given important results. We consider that this method would be useful and interesting in applying to cluster configurations of both different nuclei and ${}^9Be$.

References

1. K. Ikeda, T. Myo, K. Kato et al., Di-neutron clustering and deuteron-like tensor correlation in nuclear structure focusing on ${}^{11}Li$. arXiv:nucl-th/1007.2474v2
2. W. von Oertzen, M. Freer, Y. Kanada-En'yo, Nuclear clusters and nuclear molecules. Phys. Rep. **432**, 43–113 (2006). doi:10.1016/j.physrep.2006.07.001
3. Y. Kanada-En'yo, M. Kimura, F. Kobayashi et al., Cluster structures in stable and unstable nuclei. Nucl. Sci. Tech. **26**, S20501 (2015). doi:10.13538/j.1001-8042/nst.26.S20501
4. Y.A. Lashko, G.F. Filippov, V.S. Vasilevsky, Microscopic three-cluster model of ${}^{10}Be$. Nucl. Phys. A **958**, 78–100 (2017). doi:10.1016/j.nuclphysa.2016.11.004
5. M. Freer, A.C. Merchant, Developments in the study of nuclear clustering in light even-even nuclei. J. Phys. G Nucl. Part. Phys. **23**, 261–323 (1997). doi:10.1088/0954-3899/23/3/002
6. M. Freer, The clustered nucleus—cluster structures in stable and unstable nuclei. Rep. Prog. Phys. **70**, 2149–2210 (2007). doi:10.1088/0034-4885/70/12/R03

7. F. Hoyle, On nuclear reactions occuring in very hot STARS.I. the synthesis of elements from carbon to nickel. Astrophys. J. (Suppl.) **1**, 121 (1954). doi:10.1086/190005
8. Z.H. Yang, Y.L. Ye, Z.H. Li et al., Helium–helium clustering states in ^{12}Be . Phys. Rev. C **91**, 024304 (2015). doi:10.1103/PhysRevC.91.024304
9. E.F. Zhou, J.M. Yao, Z.P. Li et al., Anatomy of molecular structures in ^{20}Ne . Phys. Lett. B **753**, 227–231 (2016). doi:10.1016/j.physletb.2015.12.028
10. M. Aygun, A comprehensive study on the internal structure and the density distribution of ^{12}Be . Rev. Mex. Fis. **62**, 336–343 (2016)
11. S.M. Lukyanov, M.N. Harakeh, M.A. Naumenko et al., Some Insights into cluster structure of ^{9}Be from ^{3}He $+^{9}$Be reaction. World J. Nucl. Sci. Technol. **5**, 265–273 (2015). doi:10.4236/wjnst.2015.54026
12. A.G. Camacho, P.R.S. Gomes, J. Lubian et al., Simultaneous optical model analysis of elastic scattering, fusion, and breakup for the ^{9}Be $+^{144}$Sm system at near-barrier energies. Phys. Rev. C **77**, 054606 (2008). doi:10.1103/PhysRevC.77.054606
13. Y. Sert, R. Yegin, H. Doğan, A theoretical investigation of ^{9}Be $+^{27}$Al reaction: phenomenological and microscopic model approximation. Indian J. Phys. **89**, 1093–1100 (2015). doi:10.1007/s12648-015-0685-9
14. S. Hossain, M.N.A. Abdullah, M.Z. Rahman et al., Non-monotonic potentials for ^{6}Li elastic scattering at 88 MeV. Phys. Scr. **87**, 015201 (2013). doi:10.1088/0031-8949/87/01/015201
15. M.E. Farid, M.A. Hassanain, Density-independent folding analysis of the ^{6,7}Li elastic scattering at intermediate energies. Nucl. Phys. A **678**, 39–75 (2000). doi:10.1016/S0375-9474(00)00313-4
16. S.A. Seyyedi, H. Golnarkar, Nuclear matter incompressibility effect on the cross section of fusion reactions with a weakly bound projectile. arXiv:nucl-th/1501.04460v1
17. Reference Input Parameter Library (RIPL-3). http://www-nds.iaea.org/RIPL-3/
18. I.J. Thompson, Coupled reaction channels calculations in nuclear-physics. Comput. Phys. Rep. **7**, 167 (1988). doi:10.1016/0167-7977(88)90005-6
19. D. Baye, L. Desorgher, D. Guillain et al., Double-folding interaction for ^{6}He $+\alpha$ scattering. Phys. Rev. C **54**, 2563 (1996). doi:10.1103/PhysRevC.54.2563
20. A.K. Chaudhuri, Density distribution of ^{11}Li and proton elastic scattering from ^{9}Li and ^{11}Li . Phys. Rev. C **49**, 1603 (1994). doi:10.1103/PhysRevC.49.1603
21. R.A. Rego, Closed-form expressions for cross sections of exotic nuclei. Nucl. Phys. A **581**, 119–130 (1995). doi:10.1016/0375-9474(94)00424-L
22. A.Y. Abul-Magd, M. El-Nadi, Optical model parameters for composite particles. Prog. Theor. Phys. **35**, 798 (1966). doi:10.1143/PTP.35.798
23. M.F. Vineyard, J. Cook, K.W. Kemper et al., Optical potentials for the elastic scattering of ^{6}Li $+^{12}$C , ^{6}Li $+^{16}$O , and ^{7}Li $+^{12}$C . Phys. Rev. C **30**, 916 (1984). doi:10.1103/PhysRevC.30.916
24. S.C. Pieper, K. Varga, R.B. Wiringa, Quantum Monte Carlo calculations of A=9,10 nuclei. Phys. Rev. C **66**, 044310 (2002). doi:10.1103/PhysRevC.66.044310
25. K.H. Bray, M. Jain, K.S. Jayaraman et al., Elastic and inelastic scattering of protons from ^{6}Li between 25 and 45 MeV. Nucl. Phys. A **189**, 35–64 (1972). doi:10.1016/0375-9474(72)90645-8
26. F.S. Chwieroth, Y.C. Tang, D.R. Thompson, Microscopic coupled-channel study of the five-nucleon system with the resonating-group method. Phys. Rev. C **9**, 56 (1974). doi:10.1103/PhysRevC.9.56
27. P.R.S. Gomes, R.M. Anjos, C. Muri et al., Threshold anomaly with weakly bound projectiles: elastic scattering of ^{9}Be $+^{27}$Al . Phys. Rev. C **70**, 054605 (2004). doi:10.1103/PhysRevC.70.054605
28. R.M. Anjos, C. Muri, J. Lubian et al., No evidence of break-up effects on the fusion of ^{9}Be with medium-light nuclei. Phys. Lett. B **534**, 45–51 (2002). doi:10.1016/S0370-2693(02)01554-X
29. Nuclear Reaction Video, Low energy Nuclear Knowledge Base. http://nrv.jinr.ru/nrv/webnrv/elastic-scattering/reactions.php
30. M. Hugi, J. Lang, R. Müller et al., Fusion and direct reactions for strongly and weakly bound projectiles. Nucl. Phys. A **368**, 173–188 (1981). doi:10.1016/0375-9474(81)90739-9
31. M.S. Zisman, J.G. Cramer, D.A. Goldberg et al., Dominance of strong absorption in ^{9}Be $+^{28}$Si elastic scattering. Phys. Rev. C **21**, 2398 (1980). doi:10.1103/PhysRevC.21.2398
32. S.B. Moraes, P.R.S. Gomes, J. Lubian et al., Fusion and elastic scattering of ^{9}Be $+^{64}$Zn : a search of the breakup influence on these processes. Phys. Rev. C **61**, 064608 (2000). doi:10.1103/PhysRevC.61.064608
33. P.R.S. Gomes, I. Padron, E. Crema et al., Comprehensive study of reaction mechanisms for the ^{9}Be $+^{144}$Sm system at near- and sub-barrier energies. Phys. Rev. C **73**, 064606 (2006). doi:10.1103/PhysRevC.73.064606
34. P.R.S. Gomes, J. Lubian, B. Paes et al., Near-barrier fusion, breakup and scattering for the ^{9}Be $+^{144}$Sm system. Nucl. Phys. A **828**, 233–252 (2009). doi:10.1016/j.nuclphysa.2009.07.008
35. N. Yu, H.Q. Zhang, H.M. Jia et al., Unusual potential behavior for the weakly bound nucleus ^{9}Be in elastic scattering from ^{208}Pb and ^{209}Bi near the threshold. J. Phys. G Nucl. Part. Phys. **37**, 075108 (2010). doi:10.1088/0954-3899/37/7/075108
36. G.R. Satchler, W.G. Love, Folding model potentials from realistic interactions for heavy-ion scattering. Phys. Rep. **55**, 183–254 (1979). doi:10.1016/0370-1573(79)90081-4